Direct method of extracting complex refractive index from routine Fourier transform infrared reflectance/transmittance measurements

Braden Czapla[a] and Leonard Hanssen[a]

[a]Sensor Science Division, National Institute of Standards and Technology*, 100 Bureau Drive, Gaithersburg, MD 20899, USA

ABSTRACT

We describe an algorithm to extract the complex refractive index of a material from reflectance and transmittance measurements commonly taken by spectrophotometers. The algorithm combines Kramers-Kronig analysis with an inversion of Fresnel's equations to provide a direct method of solving for the refractive index which is accurate, even for weakly absorbing materials. We discuss the details of the uncertainty analysis of the algorithm. The algorithm is validated by extracting the complex refractive index of polydimethylsiloxane between 2 µm and 18 µm and comparing against existing literature.

Keywords: Reflectance, transmittance, spectrophotometry, refractive index, Kramers-Kronig, polydimethylsiloxane, PDMS

1. INTRODUCTION

Material optical properties are crucial in the design of any device which will interact with electromagnetic radiation. This includes not just optical components such as lenses, mirrors, and filters, but also any system which will emit or absorb thermal radiation. For linear, isotropic, and non-scattering media, the complex refractive index can completely describe the thermal radiation emitted by a material. Radiative heat transfer is an inherently broadband phenomenon, so broadband optical properties of materials are required to model it. In this work, we will present a numerical algorithm for extracting broadband optical properties of materials from common reflectance and transmittance measurements. The outline of this work is as follows. First in Sec. 2.1, we will discuss a technique to directly invert reflectance and transmittance to determine the complex refractive index of transmitting samples. Next in Sec. 2.2, we will describe the application of Kramers-Kronig analysis to reflectance data and cover two key innovations which improve the analysis. Then in Sec. 2.3, we discuss how these two methods may be used in tandem to form a direct method which may be applied to any material with at least two transmission bands. Finally in Sec. 3, we apply the algorithm to measurements of polydimethylsiloxane (PDMS) to extract its complex refractive index and compare the result to existing literature.

2. DIRECT DETERMINATION OF OPTICAL CONSTANTS

Throughout this work, we will define the complex refractive index, $\widetilde{n}$, as $\widetilde{n} = n + i\kappa$ where the real part, n, is commonly referred to simply as the refractive index and the imaginary part, κ, is the extinction coefficient. A number of methods exist for determining the complex refractive index from measurements of reflectance and/or transmittance.[1–9] Most attractive for their simplicity are direct methods, i.e., those which may be written $\widetilde{n} = f(R, T)$, where R and T are measured values of reflectance and transmittance. The function f varies from method to method but is a known function of R, T, and perhaps other easily accessible variables. Many direct methods involve inverting Fresnel equations, which can often be extremely sensitive to noise in the measurands.[10] In this work, we will utilize two direct methods which are less susceptible to measurement noise: an analytical solution recently put forth by Nichelatti[11] and the Kramers-Kronig relations.[12–17]

Further author information: (Send correspondence to B.C.)
B.C.: E-mail: braden.czapla@nist.gov, Telephone: +1 (301) 975-2157
L.H.: E-mail: leonard.hanssen@nist.gov, Telephone: +1 (301) 975-2344

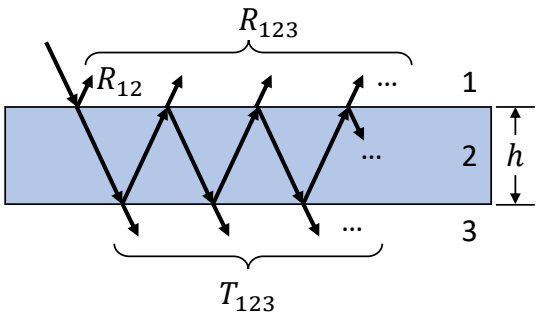

Figure 1. Schematic of measurement geometry.

2.1 Nichelatti's Method

Nichelatti examined the case of a thick slab of material with two smooth, parallel faces (see Fig. 1 for a schematic).[11] The material of interest, labeled 2, has thickness h and is embedded between two regions labeled 1 and 3. For the purposes of this work, regions 1 and 3 will be taken as vacuum. A ray of light, depicted by an arrow, impinges on the interface between regions 1 and 2. Subsequent reflections and transmissions are shown by the various daughter rays. If the initial ray is taken to have unity intensity, then the first surface reflectance is shown as R_{12}. The reflectance including all contributions from internal reflections is shown as R_{123}. Similarly, the total transmittance taking into account all internal reflections is shown as T_{123}.

Nichelatti determined a direct method of inverting Fresnel's equations for reflectance and transmittance to extract the complex refractive index. The solution is valid for thick slabs (i.e., those in which the multiple reflections of light between the parallel faces add incoherently). The key results of Nichelatti's work are

$$\kappa = \frac{\lambda}{4\pi h} \ln\left(\frac{R_{12}T_{123}}{R_{123} - R_{12}}\right) \tag{1}$$

$$n = \frac{1+R_{12}}{1-R_{12}} + \sqrt{\left(\frac{1+R_{12}}{1-R_{12}}\right)^2 - 1 - \kappa^2}\,, \tag{2}$$

where

$$R_{12} = \frac{2 + T_{123}^2 - (1-R_{123})^2 - \sqrt{(2+T_{123}^2-(1-R_{123})^2)^2 - 4R_{123}(2-R_{123})}}{2(2-R_{123})} \tag{3}$$

and λ is the wavelength. Though not explicitly written here, it is important to note that n, κ, R_{123}, T_{123}, and R_{12} are all functions of λ. Explicit formulas for the propagation of experimental uncertainty in Eqs. (1)-(3) are given in Appendix A

Recent work by Brissinger verified Nichelatti's method gives accurate results when using reflectance measurements at near-normal incidence.[18] Furthermore, Brissinger provided an estimate of the greatest extinction coefficient Nichelatti's method can accurately discern, based on the noise floor of the instrument's transmittance measurements, T_{noise}:

$$\kappa_{\max} = \frac{\lambda}{4\pi h} \ln\left[\frac{(1-R_{123})^2}{T_{\text{noise}}}\right]. \tag{4}$$

2.2 Kramers-Kronig Analysis

Kramers-Kronig analysis is a mathematical technique which takes advantage of the link between the real and imaginary parts of certain analytic functions. The theory, application, and limitations of Kramers-Kronig analysis has been documented thoroughly by various researchers.[12–17,19–24] In this work, we will apply Kramers-Kronig analysis to the Fresnel reflection coefficient. The Fresnel reflection coefficient is related to both R_{12} and $\widetilde{n}$ by

$$r = \sqrt{R_{12}}\exp(i\delta) = \frac{\widetilde{n}-1}{\widetilde{n}+1}\,, \tag{5}$$

where δ is the phase angle of r. Applying Kramers-Kronig analysis to Eq. (5), we get

$$\delta(\omega) = \frac{-\omega}{\pi}\mathcal{P}\int_0^\infty \frac{\ln\left(R_{12}(\omega')\right)}{\omega'^2-\omega^2}d\omega' \,, \tag{6}$$

where ω' is an arbitrary integration variable, $\omega = 2\pi c/\lambda$ is the angular frequency, c is the speed of light in vacuum, and $\mathcal{P}$ indicates the Cauchy principal value. Equation (6) has two important characteristics to note at this time. First, the value of the integrand is not finite for $\omega' = \omega$. Indeed, that is exactly why we must take the Cauchy principal value of the integral. Second, the value of the phase at any single frequency is impacted by the value of reflectance at all frequencies. To evaluate Eq. (6), for an arbitrary sample, even over a finite range, we would need to measure the value of R_{12} at every frequency.

To overcome these two challenges, we draw on innovations from past works. First, we use an integral which evaluates to the same value but has an integrand which is always finite. That new integral has previously been described by Yamamoto and Masui[25] and is given by

$$\delta(\omega) = \frac{-\omega}{\pi}\int_0^\infty \frac{\ln\left(R_{12}(\omega')\right)-\ln\left(R_{12}(\omega)\right)}{\omega'^2-\omega^2}d\omega' \,. \tag{7}$$

Second, we apply a technique innovated by Roessler[22–24] to address the finite measurement range of their data. Many past works have used extrapolation procedures to artificially extend the range of their data, such as assuming the value of R_{12} is constant outside the measured range[26] or fitting a model to the ends of the measured data and extrapolating it outward.[27–30] Roessler's technique, however, requires only data within the measurement range. Although the integral for δ used by Roessler was not identical to Eq. (7), their technique may be applied to Eq. (7) as well. Roessler broke the integral into three parts and treated each separately. Doing so, we get

$$\delta(\omega) = \alpha(\omega) + \beta(\omega) + \gamma(\omega) \,, \tag{8}$$

where

$$\alpha(\omega) = \frac{-\omega}{\pi}\int_0^{\omega_{\text{lower}}} \frac{\ln\left(R_{12}(\omega')\right)-\ln\left(R_{12}(\omega)\right)}{\omega'^2-\omega^2}d\omega' \tag{9}$$

$$\beta(\omega) = \frac{-\omega}{\pi}\int_{\omega_{\text{lower}}}^{\omega_{\text{upper}}} \frac{\ln\left(R_{12}(\omega')\right)-\ln\left(R_{12}(\omega)\right)}{\omega'^2-\omega^2}d\omega' \tag{10}$$

$$\gamma(\omega) = \frac{-\omega}{\pi}\int_{\omega_{\text{upper}}}^{\infty} \frac{\ln\left(R_{12}(\omega')\right)-\ln\left(R_{12}(\omega)\right)}{\omega'^2-\omega^2}d\omega' \tag{11}$$

and ω_{upper} and ω_{lower} are the upper and lower frequency bounds of the experimental data, respectively. Equation (10) may be evaluated directly from the experimental data using numerical integration. Integrating by parts, we evaluate to Eq. (9) and (11) to get

$$\alpha(\omega) = \left[C_\alpha(\omega) + \frac{\ln\left[R_{12}(\omega)\right]}{2\pi}\right]\ln\left(\frac{\omega-\omega_{\text{lower}}}{\omega+\omega_{\text{lower}}}\right) \tag{12}$$

$$\gamma(\omega) = \left[C_\gamma(\omega) - \frac{\ln\left[R_{12}(\omega)\right]}{2\pi}\right]\ln\left(\frac{\omega_{\text{upper}}-\omega}{\omega_{\text{upper}}+\omega}\right) , \tag{13}$$

where $C_\alpha(\omega)$ and $C_\gamma(\omega)$ are weakly varying functions within $[\omega_{\text{lower}}, \omega_{\text{upper}}]$.

By approximating $C_\alpha(\omega)$ and $C_\gamma(\omega)$ as constant within the measurement range, the problem of needing information from all frequencies outside the measurement range is reduced to a problem of needing the value of the phase of r at two frequencies within the measurement range. With that information, we may solve for C_α and C_γ directly. For any sample which transmits at two frequencies and meets the assumptions of the method, we may apply Nichelatti's method to obtain the values of n and κ and thus obtain δ at those two frequencies from Eq. (5).

2.3 Numerical Algorithm

In this work, we propose the following algorithm for measuring the complex refractive index:

1. Measure R_{123} and T_{123} over as broad of a spectral range as is feasible. Confirm that two transmission bands exist in the spectrum of T_{123}.
2. Use Eq. (3) to compute R_{12} from R_{123} and T_{123}.
3. Apply Nichelatti's method to directly solve for n and κ at all frequencies for which the value of T_{123} is statistically distinguishable from zero, as determined by the uncertainty of the measurement.
4. Compute the phase of r using n and κ at two frequencies. In practice, the location of these two frequencies is best when R_{12} is flat at each location and the frequencies enclose the portion of spectrum which does not transmit.
5. Compute $\beta(\omega)$ using Eq. (10) and numerical integration.
6. Solve for C_α and C_γ using Eqs. (8), (10), (12), (13), and the two known values of phase.
7. Compute δ for all values of frequency. Use Eq. (5) to solve for $\widetilde{n}$.
8. For any frequency for which the value of n and κ has been computed using both Nichelatti's method and Kramers-Kronig analysis, choose the value with a smaller uncertainty. In many cases, this tends to mean choosing values of κ from Nichelatti's method and values of n from Kramers-Kronig analysis. See Appendix A for discussion of uncertainty for each method.

3. REFRACTIVE INDEX OF PDMS

In order to validate this method, we applied it to measurements of PDMS and compared the results against a recent work which characterized the infrared refractive index using infrared ellipsometry.[31] Two samples of PDMS, henceforth referred to as Sample 1 and Sample 2, were prepared with thicknesses (0.11 ± 0.02) mm and (1.91 ± 0.02) mm, respectively ($k = 2$ expanded uncertainty). The reflectance and transmittance of each sample was measured between approximately 2 µm and 18 µm using a custom Fourier transform infrared spectrophotometer equipped with an integrating sphere.[32–36] The resulting measured values are shown in Fig. 2. Also shown are the computed values of R_{12} and the $k = 2$ expanded uncertainties for each quantity. Sample 1, which is much thinner, has transmission bands between approximately 2 µm and 8 µm and between approximately 14 µm and 18 µm. Sample 2, however, only has transmission bands for wavelengths less than about 5 µm. It is important to note that R_{12} computed from both samples' measurements match within the expanded uncertainty, validating Eq. (3).

The algorithm in Sec. 2.3 was then applied to the data in Fig. 2, the results of which are presented in Fig. 3. C_α and C_γ were determined by using the complex refractive index obtained from Nichelatti's method at 3.44 µm and 15.25 µm. The result compares favorably to that of Ref. 31. For most wavelengths, the difference in n falls within the expanded uncertainties of the two methods. At short wavelengths, κ differs significantly in two wavelength bands. The differences between the two works should be explored further in future work. The uncertainty from this work was determined for Nichelatti's method by the explicit formulas in Appendix A and by a Monte Carlo simulation for Kramers-Kronig analysis. The computed uncertainties are generally lower or equal to that from Ref. 31.

4. CONCLUSION

We implemented an algorithm for determining the complex refractive index of a material over a broad spectral range from spectrophotometric measurements. We validated the algorithm by computing the complex refractive index of PDMS between 2 µm and 18 µm and comparing the result against existing literature. Our results match the existing literature for most wavelengths and generally have lower or equal uncertainties, proving the algorithm is a powerful tool for analyzing commonly recorded reflectance and transmittance measurements.

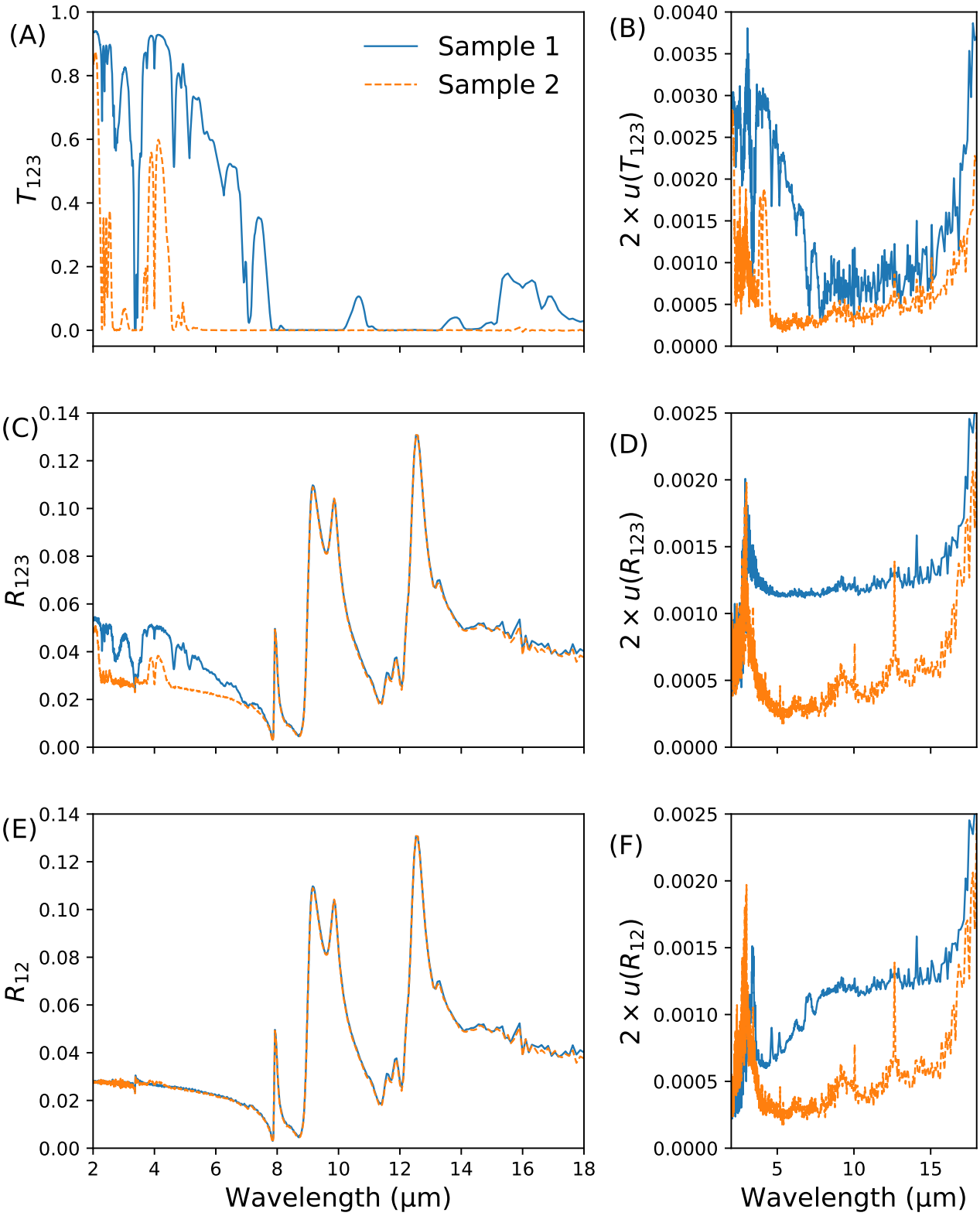

Figure 2. Measured reflectance/transmittance, calculated first surface reflectance, and associated uncertainties.

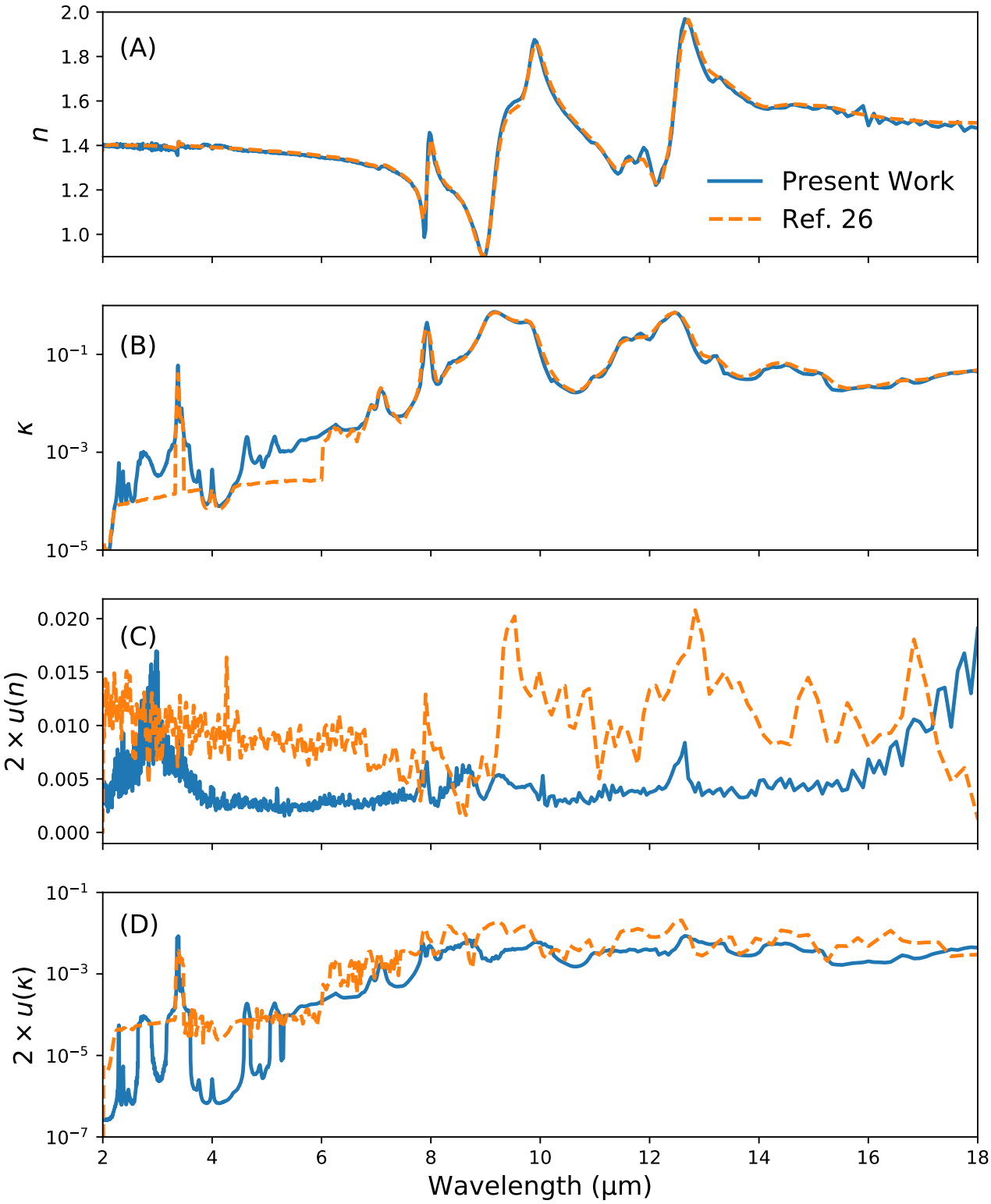

Figure 3. Complex refractive index of PDMS and associated uncertainties.

Future work in this area should determine a more rigorous way of selecting the most accurate and lowest uncertainty refractive index value when multiple values are determined, either by different samples or different methods. Further, better approximations for $C_\alpha(\omega)$ and $C_\beta(\omega)$ should be investigated. Finally, the best algorithm for numerically computing $\beta(\omega)$ should be determined to improve accuracy and uncertainty.

APPENDIX A. UNCERTAINTY ANALYSIS

A.1 Nichelatti's Method

Starting from the measurement equations

$$\kappa = \frac{\lambda}{4\pi h}\ln\left(\frac{R_{12}T_{123}}{R_{123}-R_{12}}\right) \tag{1 revisited}$$

$$n = \frac{1+R_{12}}{1-R_{12}} + \sqrt{\left(\frac{1+R_{12}}{1-R_{12}}\right)^2 - 1 - \kappa^2}\,, \tag{2 revisited}$$

$$R_{12} = \frac{2+T_{123}^2-(1-R_{123})^2 - \sqrt{(2+T_{123}^2-(1-R_{123})^2)^2 - 4R_{123}(2-R_{123})}}{2(2-R_{123})}\,, \tag{3 revisited}$$

we can write the Taylor approximation for uncorrelated parameters as

$$u\left(R_{12}\right) = \sqrt{\left(\frac{\partial R_{12}}{\partial R_{123}}\right)^2 u^2\left(R_{123}\right) + \left(\frac{\partial R_{12}}{\partial T_{123}}\right)^2 u^2\left(T_{123}\right)} \tag{14}$$

$$u\left(\kappa\right) = \sqrt{\left(\frac{\partial \kappa}{\partial R_{123}}\right)^2 u^2\left(R_{123}\right) + \left(\frac{\partial \kappa}{\partial T_{123}}\right)^2 u^2\left(T_{123}\right) + \left(\frac{\partial \kappa}{\partial h}\right)^2 u^2\left(h\right) + \left(\frac{\partial \kappa}{\partial \lambda}\right)^2 u^2\left(\lambda\right)} \tag{15}$$

$$u\left(n\right) = \sqrt{\left(\frac{\partial n}{\partial R_{123}}\right)^2 u^2\left(R_{123}\right) + \left(\frac{\partial n}{\partial T_{123}}\right)^2 u^2\left(T_{123}\right) + \left(\frac{\partial n}{\partial h}\right)^2 u^2\left(h\right) + \left(\frac{\partial n}{\partial \lambda}\right)^2 u^2\left(\lambda\right)}\,, \tag{16}$$

where $u\left(x\right)$ is the standard uncertainty of any variable x. Evaluating the partial derivatives in Eqs. (14)-(16), we get

$$\frac{1}{R_{12}}\frac{\partial R_{12}}{\partial R_{123}} = \frac{(1-R_{123})^3 + (1-R_{123})T_{123}^2 + \sqrt{(1-R_{123})^4 + 2(1+R_{123}(2-R_{123}))T_{123}^2 + T_{123}^4}}{R_{123}(2-R_{123})\sqrt{(1+T_{123}^2+R_{123}(2-R_{123}))^2 - 4R_{123}(2-R_{123})}} \tag{17}$$

$$\frac{1}{R_{12}}\frac{\partial R_{12}}{\partial T_{123}} = \frac{-2T_{123}}{\sqrt{(1+T_{123}^2+R_{123}(2-R_{123}))^2 - 4R_{123}(2-R_{123})}} \tag{18}$$

$$\frac{\partial \kappa}{\partial R_{123}} = \frac{\lambda}{4\pi h}\left(\frac{R_{123}\left(\frac{1}{R_{12}}\frac{\partial R_{12}}{\partial R_{123}}\right) - 1}{R_{123}-R_{12}}\right) \tag{19}$$

$$\frac{\partial \kappa}{\partial T_{123}} = \frac{\lambda}{4\pi h}\left(\frac{R_{123}\left(\frac{1}{R_{12}}\frac{\partial R_{12}}{\partial T_{123}}\right)T_{123} + (R_{123}-R_{12})}{(R_{123}-R_{12})\,T_{123}}\right) \tag{20}$$

$$\frac{\partial \kappa}{\partial h} = -\frac{\kappa}{h} \tag{21}$$

$$\frac{\partial \kappa}{\partial \lambda} = \frac{\kappa}{\lambda} \tag{22}$$

$$\frac{\partial n}{\partial R_{123}} = \left(\frac{2R_{12}}{(1-R_{12})^2}\right)\left(\frac{1}{R_{12}}\frac{\partial R_{12}}{\partial R_{123}}\right) + \frac{\left(\frac{1+R_{12}}{1-R_{12}}\right)\left(\frac{2R_{12}}{(1-R_{12})^2}\right)\left(\frac{1}{R_{12}}\frac{\partial R_{12}}{\partial R_{123}}\right) - \kappa\frac{\partial \kappa}{\partial R_{123}}}{\sqrt{2\left(\frac{2R_{12}}{(1-R_{12})^2}\right) - \kappa^2}} \tag{23}$$

$$\frac{\partial n}{\partial T_{123}} = \left(\frac{2R_{12}}{(1-R_{12})^2}\right)\left(\frac{1}{R_{12}}\frac{\partial R_{12}}{\partial T_{123}}\right) + \frac{\left(\frac{1+R_{12}}{1-R_{12}}\right)\left(\frac{2R_{12}}{(1-R_{12})^2}\right)\left(\frac{1}{R_{12}}\frac{\partial R_{12}}{\partial T_{123}}\right) - \kappa\frac{\partial \kappa}{\partial T_{123}}}{\sqrt{2\left(\frac{2R_{12}}{(1-R_{12})^2}\right) - \kappa^2}} \tag{24}$$

$$\frac{\partial n}{\partial h} = -\frac{\kappa\frac{\partial \kappa}{\partial h}}{\sqrt{2\left(\frac{2R_{12}}{(1-R_{12})^2}\right) - \kappa^2}} \tag{25}$$

$$\frac{\partial n}{\partial \lambda} = -\frac{\kappa\frac{\partial \kappa}{\partial \lambda}}{\sqrt{2\left(\frac{2R_{12}}{(1-R_{12})^2}\right) - \kappa^2}}\,. \tag{26}$$

A.2 Kramers-Kronig Analysis

The uncertainty of δ is dependent on the integration algorithm and the form of the integral used. i.e. using Eq. (6), Eq. (7), or some other equivalent integral. Here we will examine the propagation of the uncertainty of δ into values of n and κ.

Starting from the measurement equations

$$n = \frac{1-R_{12}}{1+R_{12}-2\sqrt{R_{12}}\cos\delta} \tag{27}$$

$$\kappa = \frac{2\sqrt{R_{12}}\sin\delta}{1+R_{12}-2\sqrt{R_{12}}\cos\delta}\,, \tag{28}$$

we can write the Taylor approximation for uncorrelated parameters as

$$u\left(n\right) = \sqrt{\left(\frac{\partial n}{\partial R_{12}}\right)^2 u^2\left(R_{12}\right) + \left(\frac{\partial n}{\partial \delta}\right)^2 u^2\left(\delta\right)} \tag{29}$$

$$u\left(\kappa\right) = \sqrt{\left(\frac{\partial \kappa}{\partial R_{12}}\right)^2 u^2\left(R_{12}\right) + \left(\frac{\partial \kappa}{\partial \delta}\right)^2 u^2\left(\delta\right)}\,. \tag{30}$$

Evaluating the partial derivatives in Eqs. (29) and (30), we get

$$\frac{1}{n}\frac{\partial n}{\partial R_{12}} = \frac{(1+R_{12})\cos\delta - 2\sqrt{R_{12}}}{\sqrt{R_{12}}(1-R_{12})(1+R_{12}-2\sqrt{R_{12}}\cos\delta)} \tag{31}$$

$$\frac{1}{n}\frac{\partial n}{\partial \delta} = \frac{-2\sqrt{R_{12}}\sin\delta}{1+R_{12}-2\sqrt{R_{12}}\cos\delta} \tag{32}$$

$$\frac{1}{\kappa}\frac{\partial \kappa}{\partial R_{12}} = \frac{1-R_{12}}{2R_{12}(1+R_{12}-2\sqrt{R_{12}}\cos\delta)} \tag{33}$$

$$\frac{1}{\kappa}\frac{\partial \kappa}{\partial \delta} = \frac{(1+R_{12})\cos\delta - 2\sqrt{R_{12}}}{\sin\delta(1+R_{12}-2\sqrt{R_{12}}\cos\delta)}\,. \tag{34}$$

The explicit uncertainty formulas for n and κ reveal a weakness of the Kramers-Kronig approach: it can amplify uncertainty of the measurands. For weakly absorbing materials (small κ which implies small δ), the relative standard uncertainty of κ, $u(\kappa)/\kappa$, grows to infinity. For the same case, the relative standard uncertainty of n can actually reduce that of R_{12}. For $\delta \to 0$, $u(n)/n = [\sqrt{R_{12}}/(1-R_{12})][u(R_{12})/R_{12}]$. Therefore the relative standard error of n will be less than that of R_{12} for all values of R_{12} less than $3/2 - \sqrt{5}/2 \approx 0.38$. That corresponds to highly transparent materials with refractive indices less than approximately 4.24.

ACKNOWLEDGMENTS

The authors would like to acknowledge Professor Qiu Jun for providing the uncertainty data from Ref. 31.

REFERENCES

[1] Verleur, H. W., "Determination of optical constants from reflectance or transmittance measurements on bulk crystals or thin films," *J. Opt. Soc. Am.* **58**(10), 1356–1364 (1968).

[2] Querry, M. R., "Direct Solution of the Generalized Fresnel Reflectance Equations," *J. Opt. Soc. Am.* **59**, 876 (7 1969).

[3] Kolb, D. M., "Determination of the Optical Constants of Solids by Reflectance-Ratio Measurements at Non-Normal Incidence," *J. Opt. Soc. Am.* **62**, 599 (4 1972).

[4] Miller, R. F., Julien, L. S., and Taylor, A. J., "A new computational method of obtaining optical constants from reflectance ratio measurements," *J. Phys. D Appl. Phys.* **5**, 318 (12 1972).

[5] Miller, R. F., Hasan, W., and Julien, L. S., "A general procedure for evaluating optical constants from functions of reflectance at two angles of incidence," *J. Phys. D Appl. Phys.* **7**, 309 (4 1974).

[6] Azzam, R. M. A., "Explicit determination of the complex refractive index of an absorbing medium from reflectance measurements at and near normal incidence," *J. Opt. Soc. Am.* **72**, 1439 (10 1982).

[7] Vartiainen, E., Peiponen, K. E., and Asakura, T., "Maximum entropy model in reflection spectra analysis," *Opt. Commun.* **89**, 37–40 (4 1992).

[8] Palmer, K. F., Williams, M. Z., and Budde, B. A., "Multiply subtractive Kramers–Kronig analysis of optical data," *Appl. Opt.* **37**, 2660 (5 1998).

[9] Kuzmenko, A. B., "Kramers–Kronig constrained variational analysis of optical spectra," *Rev. Sci. Instrum.* **76**, 083108 (8 2005).

[10] Hunter, W. R., "Errors in using the Reflectance vs Angle of Incidence Method for Measuring Optical Constants," *J. Opt. Soc. Am.* **55**, 1197 (10 1965).

[11] Nichelatti, E., "Complex refractive index of a slab from reflectance and transmittance: analytical solution," *J. Opt. A Pure Appl. Op.* **4**, 306 (7 2002).

[12] Kramers, H. A., "La diffusion de la lumière par les atomes," in [*Atti Congressi Internazionale Fisica da Luigi Volta (Transactions of Volta Centenary Congress in Physics)*], **2**, 545–557 (1927).

[13] de Ludwig Kronig, R., "On the Theory of Dispersion of X-Rays," *J. Opt. Soc. Am.* **12**, 547 (6 1926).

[14] Bechhoefer, J., "Kramers–Kronig, Bode, and the meaning of zero," *Am. J. Phys.* **79**, 1053–1059 (10 2011).

[15] Peiponen, K.-E. and Saarinen, J. J., "Generalized Kramers–Kronig relations in nonlinear optical- and THz-spectroscopy," *Rep. Prog. Phys.* **72**, 056401 (4 2009).

[16] Grosse, P. and Offermann, V., "Analysis of reflectance data using the Kramers-Kronig Relations," *Appl. Phys. A* **52**, 138–144 (2 1991).

[17] Yamamoto, K. and Ishida, H., "Optical theory applied to infrared spectroscopy," *Vib. Spectrosc.* **8**, 1–36 (11 1994).

[18] Brissinger, D., "Complex refractive index of polycarbonate over the UV-Vis-IR region from 0.2 to 3 μm," *Appl. Opt.* **58**, 1341 (2 2019).

[19] Sharnoff, M., "Validity Conditions for the Kramers-Kronig Relations," *Am. J. Phys.* **32**, 40–44 (1 1964).

[20] Robinson, T. S., "Optical Constants by Reflection," *Proc. Phys. Soc. B* **65**(11), 910 (1952).

[21] Leveque, G., "Reflectivity extrapolations in Kramers-Kronig analysis," *J. Phys. C* **10**, 4877–4888 (12 1977).

[22] Roessler, D. M., "Kramers-Kronig analysis of reflection data," *Br. J. Appl. Phys.* **16**, 1119–1123 (8 1965).

[23] Roessler, D. M., "Kramers-Kronig analysis of non-normal incidence reflection," *Br. J. Appl. Phys.* **16**, 1359–1366 (9 1965).

[24] Roessler, D. M., "Kramers-Kronig analysis of reflectance data: III. Approximations, with reference to sodium iodide," *Br. J. Appl. Phys.* **17**, 1313–1317 (10 1966).

[25] Yamamoto, K. and Masui, A., "Complex Refractive Index Determination of Bulk Materials from Infrared Reflection Spectra," *Appl. Spectrosc.* **49**, 639–644 (5 1995).

[26] Gottlieb, M., "Optical Properties of Lithium Fluoride in the Infrared," *J. Opt. Soc. Am.* **50**, 343 (4 1960).

[27] Jahoda, F. C., "Fundamental absorption of barium oxide from its reflectivity spectrum," *Phys. Rev.* **107**, 1261–1265 (9 1957).

[28] Thomas, D. G. and Hopfield, J. J., "Exciton Spectrum of Cadmium Sulfide," *Phys. Rev.* **116**, 573–582 (11 1959).

[29] Spitzer, W. G. and Kleinman, D. A., "Infrared lattice bands of quartz," *Phys. Rev.* **121**, 1324–1335 (3 1961).

[30] Andermann, G., Caron, A., and Dows, D. A., "Kramers-Kronig Dispersion Analysis of Infrared Reflectance Bands," *J. Opt. Soc. Am.* **55**, 1210 (10 1965).

[31] Zhang, X., Qiu, J., Zhao, J., Li, X., and Liu, L., "Complex refractive indices measurements of polymers in infrared bands," *J. Quant. Spectrosc. Ra.* **252**, 107063 (9 2020).

[32] Hanssen, L. M., Kaplan, S. G., and Datla, R., "Infrared optical properties of materials," *NIST Special Publication* **250-94** (2015).

[33] Hanssen, L. M. and Kaplan, S., "Infrared diffuse reflectance instrumentation and standards at NIST," in [*Analytica Chimica Acta*], **380**, 289–302, Elsevier (2 1999).

[34] Hanssen, L. M. and Snail, K. A., "Integrating spheres for mid- and near infrared reflection spectroscopy," in [*Handbook of Vibrational Spectroscopy*], Chalmers, J. M. and Griffiths, P. R., eds., 1175–1192, John Wiley & Sons, Ltd (2002).

[35] Hanssen, L. M., Prokhorov, A. V., and Khromchenko, V. B., "Specular baffle for improved infrared integrating sphere performance," in [*Optical Diagnostic Methods for Inorganic Materials III*], Hanssen, L. M., ed., **5192**, 101, SPIE (11 2003).

[36] Hanssen, L., "Integrating-sphere system and method for absolute measurement of transmittance, reflectance, and absorptance of specular samples," *Appl. Opt.* **40**, 3196 (7 2001).